Article

Molecular Catenation *via* Metal-Directed Self-Assembly and π-Donor/π-Acceptor Interactions: Efficient One-Pot Synthesis, Characterization, and Crystal Structures of [3]Catenanes Based on Pd or Pt Dinuclear Metallocycles

Vctor Blanco, Marcos Chas, Dolores Abella, Carlos Peinador, and Jos M. Quintela

J. Am. Chem. Soc., **2007**, 129 (45), 13978-13986• DOI: 10.1021/ja074721a • Publication Date (Web): 23 October 2007

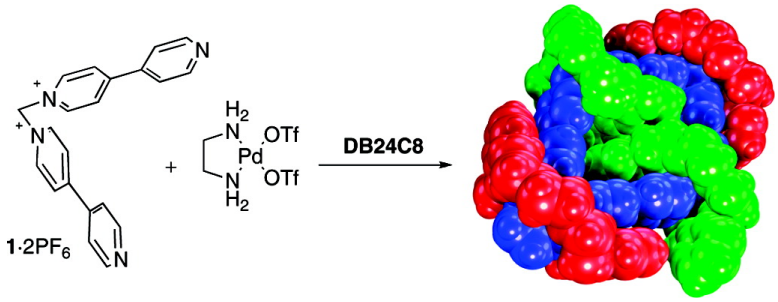

More About This Article

Additional resources and features associated with this article are available within the HTML version:

- Supporting Information
- Links to the 7 articles that cite this article, as of the time of this article download
- Access to high resolution figures
- Links to articles and content related to this article
- Copyright permission to reproduce figures and/or text from this article

View the Full Text HTML

J|A|C|S
ARTICLES
Published on Web 10/23/2007

Molecular Catenation *via* Metal-Directed Self-Assembly and π-Donor/π-Acceptor Interactions: Efficient One-Pot Synthesis, Characterization, and Crystal Structures of [3]Catenanes Based on Pd or Pt Dinuclear Metallocycles

Víctor Blanco, Marcos Chas, Dolores Abella, Carlos Peinador,* and José M. Quintela*

Contribution from the Departamento de Química Fundamental, Facultad de Ciencias, Universidade da Coruña, Campus A Zapateira, 15071, A Coruña, Spain

Received June 27, 2007; E-mail: capeveqo@udc.es; jqqoqf@udc.es

Abstract: Dinuclear square metallocycles **3a,b** assemble spontaneously when M(en)$(OTf)_2$ (M = Pd, Pt) and a 4,4′-bipyridinium ligand are mixed in acetonitrile. Six new [3]catenanes were prepared in good yields by thermodynamically driven self-assembly reaction of molecular squares **3a,b** and π-complementary dioxoaryl cyclophanes. Single-crystal X-ray analyses of the [3]catenanes revealed the insertion of two aromatic units inside the metallocycle cavity. The structures are stabilized by means of a combination of $\pi-\pi$ stacking, [C−H···π] interactions, and [C−H···O] hydrogen bonds. [3]Catenane (**DB24C8**)$_2$-(**3a**) showed in solid-state two external **DB24C8** rings positioned over the Pd(en) corners, which are held in position by [N−H···O] hydrogen bonds. Furthermore, formation of catenane (**DB24C8**)$_2$-(**3a**) can be switched off and on in a controllable manner by successive addition of KPF_6 and 18-crown-6.

Introduction

Catenanes are molecular systems composed of two or more interlocked macrocycles.[1] These molecules, apart from their intrinsic beauty, display interesting physical properties, and some can be considered as molecular machines or motors.[2] The synthesis of catenanes has been one of the topics where supramolecular chemistry has obtained numerous successes. The use of self-assembly processes guided by noncovalent forces facilitates the preorganization of the molecular components prior to the cyclization reactions. Many [2]catenanes have been synthesized *via* π-donor/π-acceptor complexes,[3] hydrogen bond interactions,[4] anion templation,[5] or metal complexation;[6] these strategies have also been applied to higher order [*n*]catenanes formed by *n* interlocked macrocycles.[7] However, an efficient and preparative synthesis of oligocatenanes remains elusive, probably due to the difficulty of synthesizing large enough macrocycles and the formation of catenanes of lower and/or higher order. [3]Catenanes have been prepared, for example, based on hydrogen bonds between amide groups or dialkyl ammonium salts and crown ethers,[8] anion templation,[9] $\pi-\pi$ interactions,[10] and *via* coordination to metal centers.[11]

In previous works we reported a facile and efficient metal-directed self-assembly of [3]catenanes and inclusion complexes from ligands based on *N*-monoalkyl-4,4′-bipyridinium, dioxoaryl cyclophanes, and a square-planar Pd complex.[12] The successful catenation process relies on the two key issues increased acceptor character of ligands upon coordination to the palladium center and the kinetically labile palladium(II)−nitrogen bond. This process is an example of a thermodynamically controlled

(1) (a) *Molecular Catenanes, Rotaxanes and Knots*; Sauvage, J.-P., Dietrich-Buchecker, C., Eds.; Wiley-VCH: Weinheim, 1999. (b) For review articles, see: Amabilino, D. B.; Stoddart, J. F. *Chem. Rev.* **1995**, *95*, 2725. (c) Chambron, J.-C.; Dietrich-Buchecker, C.; Sauvage, J.-P. In *Templating Self-Assembly, and Self-Organisation*; Sauvage, J.-P., Hosseini, M. W., Eds.; Comprehensive Supramolecular Chemistry Vol. 9; Pergamon: New York, 1996; pp 43−83. (d) Breault, G. A.; Hunter, C. A.; Mayers, P. C. *Tetrahedron* **1999**, *55*, 5265. (e) Vögtle, F.; Dünnwald, T.; Schmidt, T. *Acc. Chem. Res.* **1996**, *29*, 451.

(2) (a) Feringa, B. L. *Molecular Switches*; Wiley-VCH: Weinheim, 2001. (b) Collier, C. P.; Mattersteig, G.; Wong, E. W.; Luo, Y.; Beverly, K.; Sampaio, J.; Raymo, F. M.; Stoddart, J. F.; Heath, J. R. *Science* **2000**, *289*, 1172. (c) Jeppesen, J. O.; Perkins, J.; Becher, J.; Stoddart, J. F. *Angew. Chem., Int. Ed.* **2001**, *40*, 1216. (d) Sauvage, J.-P. *Chem. Commun.* **2005**, 1507. (e) Balzani, V.; Venturi, M.; Credi, A. *Molecular Devices and Machines*; Wiley-VCH: Weinheim, 2003. (f) Schalley, C. A.; Lützen, A.; Albrecht, M. *Chem.—Eur. J.* **2004**, *10*, 1072. (g) Kay, E. R.; Leigh, D. A.; Zerbetto, F. *Angew. Chem., Int. Ed.* **2007**, *46*, 72.

(3) (a) Balzani, V.; Credi, A.; Langford, S. J.; Raymo, F. M.; Stoddart, J. F.; Venturi, M. *J. Am. Chem. Soc.* **2000**, *122*, 3542. (b) Tseng, H-R.; Vignon, S. A.; Celestre, P. C.; Perkins, J.; Jeppesen, J. O.; Di Fabio, A.; Ballardini, R.; Gandolfi, M. T.; Venturi, M.; Balzani, V.; Stoddart, J. F. *Chem.—Eur. J.* **2004**, *10*, 155 and references therein.

(4) (a) Leigh, D. A.; Venturini, A.; Wilson, A. J.; Wong, J. K. Y.; Zerbetto, F. *Chem.—Eur. J.* **2004**, *10*, 4960. (b) Johnston, A. G.; Leigh, D. A.; Pritchard, R. J.; Deegan, M. D. *Angew. Chem., Int. Ed.* **1995**, *34*, 1209. (c) Fustin, C. A.; Bailly, C.; Clarkson, G. J.; De Groote, P.; Galow, T. H.; Leigh, D. A.; Robertson, D.; Slawin, A. M. Z.; Wong, J. K. Y. *J. Am. Chem. Soc.* **2003**, *125*, 2200. (d) Jager, R.; Vogtle, F. *Angew. Chem., Int. Ed* **1997**, *36*, 930.

(5) Ng, K.-Y.; Cowley, A. R.; Beer, P. D. *Chem. Commun.* **2006**, 3676.

(6) (a) Sauvage, J.-P. *Acc. Chem. Res.* 1998, *31*, 611 and references therein. (b) Collin, J.-P.; Heitz, V.; Bonnet, S.; Sauvage, J.-P. *Inorg. Chem. Commun.* **2005**, *8*, 1063. (c) Chambron, J.-C.; Collin, J.-P.; Heitz, V.; Jouvenot, D.; Kern, J.-M.; Mobian, P.; Pomeranc, D.; Sauvage, J.-P. *Eur. J. Org. Chem.* **2004**, 1627. (d) Fujita, M.; Fujita, N.; Ogura, K.; Yamaguchi, K. *Nature* **1999**, *400*, 52. (e) Chas, M.; Pia, E.; Toba, R.; Peinador, C.; Quintela, J. M. *Inorg. Chem.* **2006**, *45*, 6117. (f) Abedin, T. S. M.; Thompson, L. K.; Miller, D. O. *Chem. Commun.* **2005**, 5512. (g) McArdle, C. P.; Irwin, M. J.; Jennings, M. C.; Vittal, J. J.; Puddephatt, R. J. *Chem.—Eur. J.* **2002**, *8*, 723.

(7) (a) Amabilino, D. B.; Ashton, P. R.; Reder, A. S.; Spencer, N.; Stoddart, J. F. *Angew. Chem., Int. Ed. Engl.* **1994**, *33*, 1286. For the five-stage self-assembly of a branched [7]catenane, see: (b) Amabilino, D. B.; Ashton, P. R.; Boyd, S. E.; Lee, J. Y.; Menzer, S.; Stoddart, J. F.; Williams, D. J. *Angew. Chem., Int. Ed. Engl.* **1997**, *36*, 2070.

10.1021/ja074721a CCC: $37.00

self-assembly system, a very common strategy that allows us to achieve the obtention of discrete entities with a high level of structural complexity. Although once assembled, the complex remains in equilibrium with its components and any change to equilibrium conditions can disassemble the complex. This kind of dynamic structural nature has usually lead to problems associated with characterization and isolation of many supramolecular complexes. Nevertheless, in this case, the use of stronger and more inert metal−ligand bonds should stabilize the metallomacrocyclic structures and allow their isolation and a more accurate characterization. Platinum(II) metal centers, geometrically analogous to the palladium(II) square-planar centers, afford much more inert coordination bonds with pyridine ligands. Even more, this coordination bond has a double character due to its inertness at low temperature that can be turned into lability when the temperature is increased. This dual feature was beautifully exploited by Fujita and co-workers to introduce the "molecular lock" concept.[13]

The research reported in this paper focuses on the preparation, characterization, and study of [3]catenanes based on square dinuclear metallocycles and dioxoaryl cyclophanes. The [3]-catenanes are obtained by metal-directed self-assembly of six components (1,1′-methylenebis-4,4′-bipyridinium, a dioxoaryl cyclophane, and a square-planar palladium(II) or platinum (II) complex) in a 2:2:2 ratio. The appropriate metal center should be protected so that only two *cis* positions can be involved in the complexation process. M(en)$(OTf)_2$ (M = Pd, Pt) were chosen as the two triflate ligands can be easily substituted. Thus, metal centers should react with 1,1′-methylenebis-4,4′-bipyridinium which can adopt an L-shape conformation to form a square dinuclear metallocycle. On the other hand, the formation of [3]catenanes with dioxoaryl cyclophanes should be favored by (a) $\pi-\pi$ interactions between *N*-monoalkyl-4,4′-bipyridinium systems and dioxoaryl rings and (b) hydrogen bonds between the methylene link of the ligand and oxygen atoms from the cyclophane. This type of interaction has been observed in similar systems.[14]

Chart 1. Structures Used in This Work

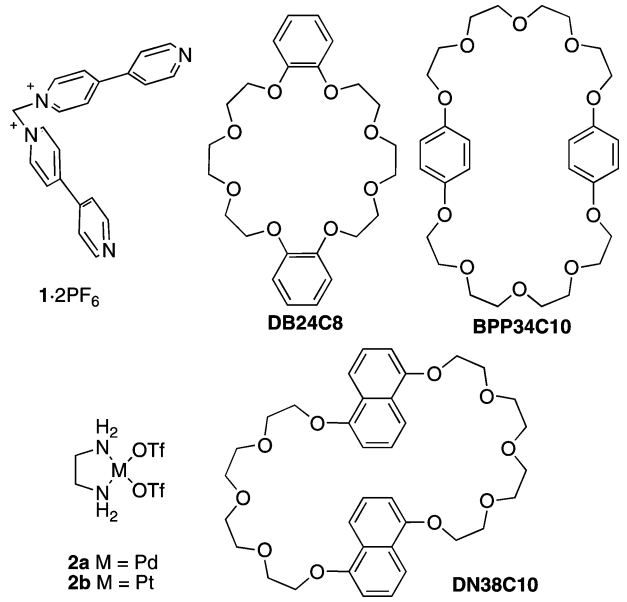

Results and Discussion

Synthesis of Bipyridinium Ligand 1·2PF_6 and Dinuclear Molecular Squares 3a,b. Molecular components used in this work are depicted in Chart 1. Ligand **1**·2PF_6 was synthesized in 91% yield by *N*-alkylation of 4,4′-bipyridine with dibromomethane. Colorless crystals of **1**·2PF_6 were isolated from solution in acetonitrile by vapor diffusion of diethyl ether, and single-crystal X-ray analysis was carried out (Table 1). The angle NCN is 112°, and the bipyridine units are nonplanar with a torsion angle between pyridines of 43°.

The addition of 1 equiv of palladium complex **2a** to a CD_3-CN solution of **1**·2PF_6 (10 mM) at room temperature gave rise to the formation of metallocycle **3a**·4PF_6·4OTf (Scheme 1). The ^{1}H and ^{13}C NMR spectra of **3a**, together with its 2D (COSY, HMBC, and HSQC) NMR spectra, provide good evidence for the formation of the macrocycle. The signals for Ca, Cb, and Cc are shifted downfield from those of the free ligand ($\Delta\delta$ = 1.6 ppm, $\Delta\delta$ = 3.1 ppm, and $\Delta\delta$ = 3.5 ppm, respectively) as a result of the formation of coordinative bonds. In the ^{1}H NMR spectrum protons Ha are shifted downfield ($\Delta\delta$ = 0.08 ppm) for the same reason. DOSY (Diffusion Ordered SpectroscopY) experiments also support the proposed structure for **3a**·4PF_6·4OTf showing for **1**·2PF_6 and **2a** significantly larger diffusion coefficients than that of **3a**·4PF_6·4OTf.[15] With the aim of supporting the formation of the molecular square, the self-assembly of the components was carried out at different concentrations and the resulting systems were monitored by ^{1}H NMR. The spectra show how the proportion of ligand **1**·2PF_6 increases as the concentration is decreased from 10 mM to 0.5 mM, the concentration at which **1**·2PF_6 is the major species (see Supporting Information).

The success of this self-assembly process is based on the lability of the N−Pd bond, but it has the disadvantage that it

(8) (a) Safarowsky, O.; Vogel, E.; Vögtle, F. *Eur. J. Org. Chem.* **2000**, 499. (b) Schwanke, F.; Safarowsky, O.; Heim, C.; Silva, G.; Vögtle, F. *Helv. Chim. Acta* **2000**, *83*, 3279. (c) Hubbard, A. L.; Davidson, G. J. E.; Patel, R. H.; Wisner, J. A.; Loeb, S. J. *Chem. Commun.* **2004**, 138. (d) Iwamoto, H.; Itoh, K.; Nagamiya, H.; Fukazawa, Y. *Tetrahedron Lett.* **2003**, *44*, 5773. (e) Leigh, D. A.; Wong, J. K. Y.; Dehez, F.; Zerbetto, F. *Nature* **2003**, *424*, 174. (f) Wang, L. Y.; Vysotsky, M. O.; Bogdan, A.; Bolte, M.; Bohmer, V. *Science* **2004**, *304*, 1312. (g) Ashton, P. R.; Baldoni, V.; Balzani, V.; Credi, A.; Hoffmann, H. D. A.; Martinez-Diaz, M.-V.; Raymo, F. M.; Stoddart, J. F.; Venturi, M. *Chem.—Eur. J.* **2001**, *7*, 3482.
(9) Sambrook, M.; Wisner, J. A.; Paul, R. L.; Cowley, A. R.; Szemes, F.; Beer, P. D. *J. Am. Chem. Soc.* **2004**, *126*, 15364.
(10) (a) Ashton, P. R.; Baldoni, V.; Balzani, V.; Claessens, C. G.; Credi, A.; Hoffmann, H. D. A.; Raymo, F. M.; Stoddart, J. F.; Venturi, M.; White, A. J. P.; Williams, D. J. *Eur. J. Org. Chem.* **2000**, 1121. (b) Chiu, S.-H.; Elizarov, A. M.; Glink, P. T.; Stoddart, J. F. *Org. Lett.* **2002**, *4*, 3561. (c) Cabezon, B.; Cao, J.; Raymo, F. M.; Stoddart, J. F.; White, A. J. P.; Williams, D. J. *Chem.—Eur. J.* **2000**, *6*, 2262. (d) Gunter, M. J.; Farquhar, S. M.; Jeynes, T. P. *Org. Biomol. Chem.* **2003**, *1*, 4097. (e) Amabilino, D. B.; Ashton, P. R.; Brown, C. L.; Cordova, E.; Godinez, L. A.; Goodnow, T. T.; Kaifer, A. E.; Newton, S. P.; Pietraszkiewicz, M.; Philp, D.; Raymo, F. M.; Reder, A. S.; Stoddart, J. F.; Williams, D. J. *J. Am. Chem. Soc.* **1995**, *117*, 1271.
(11) (a) Hori, A.; Kumazawa, K.; Kusukawa, T.; Chand, D. K.; Fujita, M.; Sakamoto, S.; Yamaguchi, K. *Chem.—Eur. J.* **2001**, *7*, 4142. (b) Sauvage, J.-P.; Weiss, J. *J. Am. Chem. Soc.* **1985**, *107*, 6108. (c) Armaroli, N.; Balzani, V.; Barigelletti, F.; De Cola, L.; Flamigni, L.; Sauvage, J.- P.; Hemmert, C. *J. Am. Chem. Soc.* **1994**, *116*, 5211. (d) Kern, J.-M.; Sauvage, J.-P.; Weidmann, J.-L. *Tetrahedron* **1996**, *52*, 10921.
(12) (a) Chas, M.; Blanco, V.; Peinador, C.; Quintela, J. M. *Org. Lett.* **2007**, *9*, 675. (b) Chas, M.; Platas-Iglesias, C.; Peinador, C.; Quintela, J. M. *Tetrahedron Lett.* **2006**, *47*, 3119. (c) Chas, M.; Abella, D.; Blanco, V.; Pía, E.; Blanco, G.; Fernández, A.; Platas-Iglesias, C.; Peinador, C.; Quintela, J. M. *Chem.—Eur. J.* **2007**, *13*, 8572−8582.
(13) (a) Fujita, M.; Ibukuro, F.; Yamaguchi, K.; Ogura, K. *J. Am. Chem. Soc.* **1995**, *117*, 4175. (b) Hori, A.; Kataoka, H.; Okano, T.; Sakamoto, S.; Yamaguchi, K.; Fujita, M. *Chem. Commun.* **2002**, 182. (c) Yamashita, K-i.; Kawano, M.; Fujita, M. *J. Am. Chem. Soc.* **2007**, *129*, 1850.
(14) (a) Loeb, S. J.; Tiburcio, J.; Vella, S. J. *Org. Lett.* **2005**, *7*, 4923. (b) Davidson, G. J. E.; Loeb, S. J.; Passaniti, P.; Silvi, S.; Credi, A. *Chem.—Eur. J.* **2006**, *12*, 3233. (c) Loeb, S. J. *Chem. Soc. Rev.* **2007**, *36*, 226.

Table 1. X-ray Crystallographic Experimental Data of **1**·2PF_6 and **DB24C8-1**·2PF_6[a]

	1·2PF_6	**DB24C8-1**·2PF_6
empirical formula	$C_{21}H_{18}F_{12}N_4P_2$	$C_{45}H_{50}F_{12}N_4O_8P_2$·3$CH_3CN$
formula weight	616.33	1188.00
crystal system	orthorhombic	monoclinic
space group	*Fdd*2	*P*2(1)/*c*
a (Å)	34.334(5)	10.7113(12)
b (Å)	10.251(5)	14.2665(17)
c (Å)	13.999(5)	36.270(4)
α (deg)	90	90
β (deg)	90	98.144(2)
γ (deg)	90	90
V (Å^3)	4927(3)	5486.6(11)
D_{calcd} (Mg m^{-3})	1.662	1.427
μ (mm^{-1})	0.287	0.179
F(000)	2480	2428
crystal size (mm)	0.31 × 0.12 × 0.07	0.50 × 0.23 × 0.16
θ limits (deg)	3.04 to 31.55	1.13 to 28.41
hkl limits	−48,30/−7,14/−14,19	−14,14/−19,19/−48,48
reflections collected	6863	73032
independent reflections	2908 [R_{int} = 0.0299]	13686 [R_{int} = 0.1105]
max and min transmission	0.9802 and 0.9162	0.9720 and 0.9159
goodness-of-fit on F^2	1.061	0.985
R [$I > 2\sigma(I)$]	$R1$ = 0.0650 $wR2$ = 0.1383	$R1$ = 0.0806 $wR2$ = 0.1880
R (all data)	$R1$ = 0.0782 $wR2$ = 0.1479	$R1$ = 0.1842 $wR2$ = 0.2479

[a] In common: Refinement method: Full-matrix least-squares on F^2. Wavelength 0.710 73 Å. Z = 4. Temperature 100(2) K.

precludes the isolation of the metallocycle **3a** from the solution. Fortunately, the more inert bond between nitrogen and platinum allowed the isolation and a more accurate characterization of the diplatinum metallocycle **3b**. As previously mentioned, this coordination bond has a double character due to its inertness at room temperature that is lost when the temperature is increased. The platinum metallocycle **3b** was synthesized in 75% yield by reaction of **1**·2PF_6 and **2b** in CH_3CN at 50 °C for 7 d. The ^{1}H and ^{13}C NMR spectra showed very similar chemical shifts to the analogous palladium complex. In contrast, dilution has no effect on the ^{1}H NMR spectrum because the molecular square is locked by the inert N−Pt bonds. High-resolution electrospray ionization mass spectrometry of **3b**·8PF_6 confirmed the structure, showing signals resulting from the loss of between three and five hexafluorophosphate anions.

Self-Assembly, NMR Study, and Solid-State Structure of Pseudorotaxanes. The nonstatistical synthesis of catenanes has followed two different strategies: the "entwining" and the "threading" strategies.[16] The former relies on the intertwining of two components before the ring-closure reaction. The second consists of the threading of a preformed cyclic component with a linear fragment with reactive ends which reacts to form a second macrocycle. The efficient formation of catenanes requires, in both approaches, a noncovalent interaction to preorganize the system.

Our strategy involves the threading of the crown ethers **BPP34C10**, **DB24C8**, and **DN38C10** (Chart 1**)** with the ligand **1**·2PF_6 and then link the resulting pseudorotaxanes with metal centers with two *cis* labile ligands to afford the [3]catenane. Thus, the following experiments were proposed to provide insights into the interactions between ligand **1**·2PF_6 and the three cyclophanes. The ^{1}H NMR spectrum of a 10 mM equimolar solution of **1**·2PF_6 and **DB24C8** shows a mixture of three species as a result of the slow equilibrium on the NMR time scale. The quantitative formation of pseudorotaxane structure is achieved with a 40% molar excess of macrocycle **DB24C8**. Interestingly, the protons Hg and Hf suffer a pronounced deshielding ($\Delta\delta$ = 0.30 ppm and $\Delta\delta$ = 0.40 ppm, respectively). Hence, it is reasonable to expect that the methylene group of **1**·2PF_6 is encircled by the macrocycle **DB24C8**. On the contrary, no changes were detected in the ^{1}H NMR spectra of **1**·2PF_6 upon the addition of **BPP34C10** or **DN38C10**.

The equimolar solutions of ligand **1**·2PF_6 and cyclic polyethers **BPP34C10**, **DB24C8**, and **DN38C10** are red, yellow, and violet colored, respectively, indicating the presence of a broad intermolecular charge-transfer band centered on 480, 356, and 535 nm, respectively. This kind of interaction has usually a very low contribution to the complex stability, but the charge-transfer bands are very useful for the determination of the association constant by means of UV−vis spectroscopy. The UV−vis titrations method was used to determine association constants in acetonitrile for the pseudorotaxanes of **1**·2PF_6 with **BPP34C10**, **DB24C8**, and **DN38C10** (K_a = 2160 ± 110, K_a = 915 ± 35, and K_a = 1292 ± 47 M^{-1}, respectively).[17] The slightly higher K_a value for **BPP34C10** pseudorotaxane compared to those of **DB24C8** and **DN38C10** presumably reflects the greater flexibility of this cyclophane to maximize the [C−H···O] hydrogen bonds.

Single crystals of the 1:1 complex between **1**·2PF_6 and **DB24C8**, suitable for X-ray analysis, were grown by vapor diffusion of ethyl ether into acetonitrile solution at room temperature. The crystal structure revealed, in agreement with ^{1}H NMR data, that the complex is stabilized by [C−H···O] hydrogen bonds between methylene protons and the oxygen atoms of the polyether chain in addition with [C−H···O] interactions between the α-CH bipyridinium hydrogens and the oxygen atoms. **DB24C8** has adopted a rare C-shaped conformation in contrast to a an S-shaped one observed in 1,2-bis-(pyridinium)ethane systems (Figure 1).[18] A $\pi-\pi$ stacking interaction is also observed between one of the aromatic rings of **DB24C8** and one of the bipyridine systems. The angle between planes is 5°, and the distance between the centroid of the **DB24C8** ring involved in the $\pi-\pi$ stacking interaction and the centroid of the bypyridinium system is 3.55 Å.

Self-Assembly, NMR Study, and Crystal Structure of [3]-Catenanes (BPP34C10)$_2$-(3a,b). The addition of 1 equiv of cyclophane **BPP34C10** to a 10 mM equimolar solution of the almost colorless ligand **1**·2PF_6 and palladium complex **2a** in CD_3CN produced an intense red color; this is related to the

(15) (a) Johnson, Jr, C. S. *Prog. Nucl. Magn. Reson.* **1999**, *34*, 203. (b) Stilbs, P. *Anal. Chem.* **1981**, *53*, 2135. (c) Morris, K. F.; Johnson, C. S., Jr. *J. Am. Chem. Soc.* **1992**, *114*, 3139. (d) For a review on the application of diffusion measurements in supramolecular chemistry, see: Cohen, Y.; Avram, L.; Frish, L. *Angew. Chem., Int. Ed.* **2005**, *44*, 520.

(16) For example, see: Dietrich-Buchecker, C.; Colasson, B.; Fujita, M.; Hori, A.; Geum, N.; Sakamoto, S.; Yamaguchi, K.; Sauvage, J. P. *J. Am. Chem. Soc.* **2003**, *125*, 5717.

(17) (a) Connors, K. A. *Binding Constants*; Wiley: New York, 1987. (b) Schneider, H.-J.; Yatsimirsky, A. K. *Principles and Methods in Supramolecular Chemistry*; John Wiley & Sons: New York, 2000.

(18) (a) Ashton, P. R.; Langford, S. J.; Spencer, N.; Stoddart, J. F.; White, A. J. P.; Williams, D. J. *Chem. Commun.* **1996**, 1387. (b) Lamsa, M.; Suorsa, T.; Pursiainen, J.; Huuskonen, J.; Rissanen, K. *Chem. Commun.* **1996**, 1443. (c) Colquhoun, H. M.; Doughty, S. M.; Stoddart, J. F.; Williams, D. J. *Angew. Chem., Int. Ed. Engl.* **1984**, *23*, 235. (d) Tiburcio, J.; Davidson, G. J. E.; Loeb, S. J. *Chem. Commun.* **2002**, 1282. For examples of an S-shaped conformation in 1,2-bis(pyridinium)ethane systems, see: (e) Loeb, S. J.; Wisner, J. A. *Chem. Commun.* **2000**, 1939. (f) Loeb, S. J.; Wisner, J. A. *Chem. Commun.* **1998**, 2757. (g) Loeb, S. J. *Chem. Commun.* **2005**, 1511.

Table 2. X-ray Crystallographic Experimental Data of Catenanes (**BPP34C10**)$_2$-(**3a**), (**DB24C8**)$_2$-(**3a**), (**DN38C10**)$_2$-(**3a**), (**DB24C8**)$_2$-(**3b**), and (**DN38C10**)$_2$-(**3b**)[a]

	(**BPP34C10**)$_2$(**3a**)	(**DB24C8**)$_2$(**3a**)	(**DN38C10**)$_2$(**3a**)	(**DB24C8**)$_2$(**3b**)	(**DN38C10**)$_2$(**3b**)
empirical formula	$C_{106}H_{132}F_{36}N_{12}O_{32}$-$P_4Pd_2S_4$·$4H_2O$·$6CH_3OH$	$C_{142}H_{180}F_{48}N_{12}O_{32}$-$P_8Pd_2$·$2.66H_2O$·$4CH_3CN$	$C_{118}H_{140}F_{48}N_{12}O_{20}$-$P_8Pd_2$·$14CH_3CN$	$C_{94}H_{116}F_{48}N_{12}O_{16}$-$P_8Pt_2$·$6H_2O$·$4CH_3CN$	$C_{118}H_{140}F_{48}N_{12}O_{20}$ P_8Pt_2·$4H_2O$·$7CH_3CN$
formulaweight	3399.53	4151.75	3993.77	3492.20	3955.78
crystal system	triclinic	rombohedric	triclinic	monoclinic	monoclinic
space group	$P\bar{1}$	$R\bar{3}$	$P\bar{1}$	$P21/c$	Cc
a (Å)	18.292(3)	37.8491(10)	15.821(4)	16.779(5)	38.981(5)
b (Å)	20.433(3)	37.8491(10)	16.112(4)	21.728(5)	21.921(5)
c (Å)	20.878(3)	33.4157(17)	19.211(4)	19.777(5)	24.767(5)
α (deg)	76.237(4)	90	111.089(4)	90	90
β (deg)	78.635(4)	90	100.668(4)	108.108(5)	125.982(5)
γ (deg)	79.900(4)	120	98.214(4)	90	90
V (Å^3)	7363(2)	41456(3)	4371.3(17)	6853(3)	17125(6)
Z	2	12	1	4	2
D_{calcd} (Mg m^{-3})	1.504	1.491	1.501	1.681	1.523
μ (mm^{-1})	0.460	0.385	0.398	2.265	1.824
F(000)	3402	19035	2002	3448	7860
crystal size (mm)	0.44 × 0.17 × 0.15	0.31 × 0.27 × 0.16	0.41 × 0.36 × 0.15	0.25 × 0.19 × 0.09	0.18 × 0.17 × 0.16
θ limits (deg)	1.02 to 28.37	0.87 to 28.34	1.18 to 28.36	1.28 to 28.75	1.13 to 24.92
hkl limits	−24,24/−27,27/−27,26	−50,50/−50,50/−44,44	−21,21/−21,21/−25,25	−22,22/−29,29/−26,26	−45,46/−25,25/−29,29
reflections collected	97592	171843	59736	150051	88110
independent reflections	35 755 [R_{int} = 0.1041]	22 653 [R_{int} = 0.2073]	21 560 [R_{int} = 0.0279]	17 694 [R_{int} = 0.0690]	28 369 [R_{int} = 0.0930]
max and min transmission	0.9341 and 0.8231	0.9409 and 0.8899	0.9427 and 0.8538	0.8221 and 0.6013	0.7590 and 0.7348
goodness-of-fit on F^2	1.340	0.918	1.037	1.034	0.971
R [$I > 2\sigma(I)$]	$R1$ = 0.1589, $wR2$ = 0.4089	$R1$ = 0.0816, $wR2$ = 0.2154	$R1$ = 0.0547, $wR2$ = 0.1493	$R1$ = 0.0882, $wR2$ = 0.2265	$R1$ = 0.0660, $wR2$ = 0.1619
R (all data)	$R1$ = 0.2740, $wR2$ = 0.4637	$R1$ = 0.1882, $wR2$ = 0.2623	$R1$ = 0.0685, $wR2$ = 0.1606	$R1$ = 0.1261, $wR2$ = 0.2581	$R1$ = 0.1005, $wR2$ = 0.1909

[a] In common: Refinement method: Full-matrix least-squares on F^2. Wavelength 0.710 73 Å. Temperature 100(2) K.

Scheme 1. Synthesis of Metallocycles

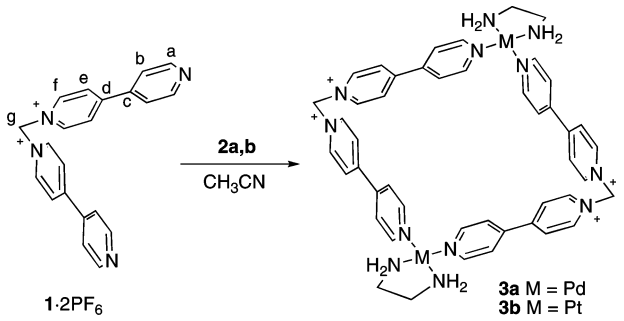

presence of a broad intermolecular charge-transfer band centered on 460 nm. The ^{1}H NMR spectrum of the mixture shows broad signals that indicate an equilibrium in solution close to coalescence. When the sample was cooled to 237 K the signals appeared well defined, so that the spectral changes originated by the formation of the [3]-(**BPP34C10**)$_2$-(**3a**) catenane can be interpreted. The ^{1}H NMR signals were unambiguously assigned by a combination of 2D NMR experiments (COSY, HSQC, and HMBC). The exchange between inside and alongside the hydroquinol rings of **BPP34C10** is slow at 237 K, resulting in all of the OCH_2 groups being anisochronous on the ^{1}H NMR time scale. Moreover, the aromatic signal of the alongside dioxoaryl rings is characteristically shifted upfield ($\Delta\delta$ = 0.65 ppm). Eight signals for the aromatic protons of the metallocycle were observed; this splitting pattern can be ascribed to the slow exchange on the NMR time scale of **BPP34C10** between bipyridine units. The mean planes of two bipyridinium systems are approximately orthogonal ($BIPY_{ort}$) to the inside dioxoaryl

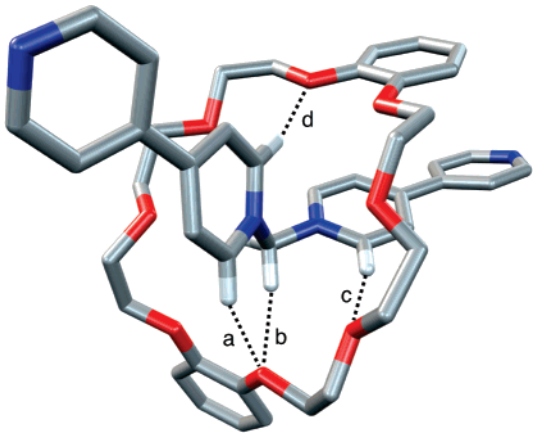

Figure 1. Crystal structure of pseudorotaxane complex between **1**·2PF$_6$ and **DB24C8** showing [C−H···O] hydrogen bonds. [H···O] and [C···O] distances and [C−H···O] angle: (a) 2.52, 3.37 Å, 149°; (b) 2.26, 3.23 Å, 167°; (c) 2.21, 3.14 Å, 167°; (d) 2.37, 3.31 Å, 168°.

rings of **BPP34C10** while the other two bipyridines are parallel ($BIPY_{par}$) to the same rings. The protons of the parallel bipyridines are shifted upfield (blue lines in Figure 2) from those of the free metallocycle **3a** as a result of the shielding effect of the cyclophane **BPP34C10**. The shielding effect is more intense in protons at the central positions of the bipyridine system ($\Delta\delta$ = −0.7 ppm for Hb′ and He′) than for the α-CH pyridine hydrogens ($\Delta\delta$ = −0.1 ppm and $\Delta\delta$ = −0.3 ppm for Ha and Hf, respectively). Thus, it is reasonable to conclude that this is the mean localization of the inside and alongside units of dioxoaryl rings. On the contrary, the protons of the $BIPY_{ort}$ are shifted downfield (red lines in Figure 2) suggesting a

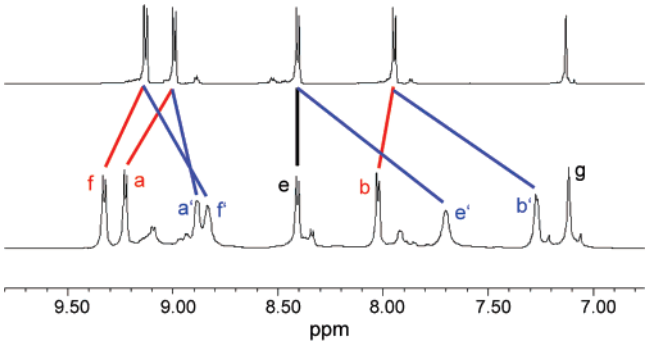

Figure 2. Partial ^{1}H NMR (CD_3CN, 500 MHz) spectra of metallocycle **3a** (top) and (**BPP34C10**)$_2$-(**3a**) at 237 K (bottom). Peak labels are defined in Scheme 1.

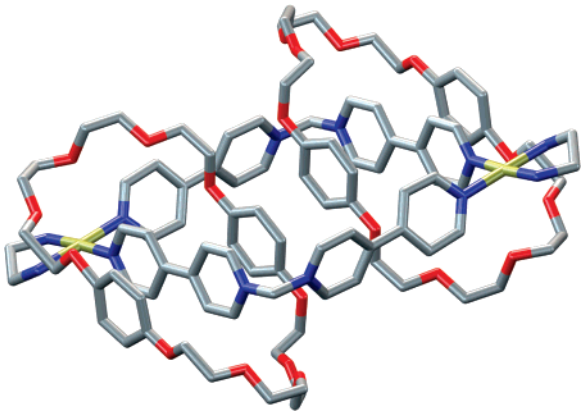

Figure 3. Crystal structure of the [3]catenane (**BPP3410**)$_2$-(**3a**). Solvents molecules, counterions, and hydrogen atoms have been omitted for clarity.

[C−H···π] interaction between the pyridine rings and the protons of the inside hydroquinol rings.[19]

The efficient catenation of metallocycle **3a** was evidenced by X-ray crystallographic analysis of single crystals obtained from a methanolic solution of **1**·2PF_6, **BPP34C10**, and **2a**. Unfortunately, crystals of [3]catenane (**BPP34C10**)$_2$-(**3a**) were of limited quality and the resulting data are somewhat poor but, nonetheless, sufficient to enable an unambiguous assignment of the molecular structure (Figure 3). The octacationic metallocycle is interlocked by two molecules of cyclophane **BPP34C10**, showing a parallel $\pi-\pi$ stacking disposition of six aromatic systems: HQ_{out}/$BIPY_{par}$/HQ_{in}/HQ_{in}/$BIPY_{par}$/HQ_{out}, where HQ_{out} and HQ_{in} stand for the alongside and the inside hydroquinol rings, respectively. The interplanar separation $HQ_{in}-HQ_{in}$ is 3.40 Å, and the distance between their centroids is 3.83 Å; hence one HQ_{in} is displaced 1.92 Å with respect to the other. The O−O vectors associated with HQ_{in} residues are tilted by 35.5° with respect to the mean plane of the metallocycle. The interplanar separations HQ_{out}···$BIPY_{par}$ and $BIPY_{par}$···HQ_{in} are 3.40 Å and 3.52 Å, respectively. Interestingly, the torsion angle of the bipyridine system involved in $\pi-\pi$ stacking interactions ($BIPY_{par}$) is much lesser than the torsion of $BIPY_{ort}$ (2° and 31°, respectively). The structure is also stabilized by means of [C−H···π] interactions between one proton of HQ_{in} and one ring of $BIPY_{ort}$; the distance between the centroid of the pyridine

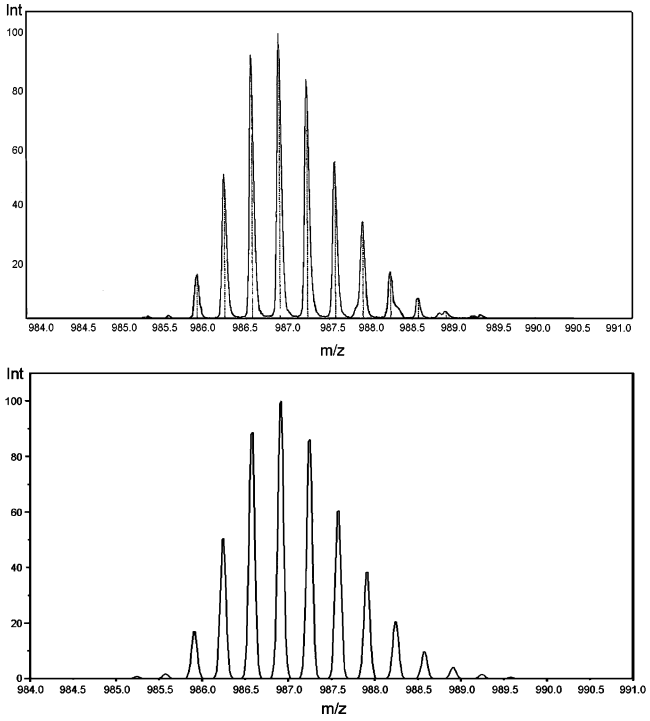

Figure 4. Observed (top) and theoretical (bottom) isotopic distribution for the fragment [(**BPP34C10**)$_2$-(**3b**) − 3PF_6]$^{+3}$.

ring and the closest C−H of the HQ_{in} is 3.06 Å and the angle 157°. The contribution of [C−H···O] interactions between the α-CH bipyridine hydrogens and the oxygen atoms of **BPP34C10** to the stabilization of catenanes and rotaxanes has been well documented in the literature.[20] In our system this type of hydrogen bond is also present ([H···O] and [C···O] distances and [C−H···O] angles for hydrogen bonds are 2.41 Å and 3.32 Å, 160°; 2.61 Å and 3.54 Å, 167°; 2.63 Å and 3.46 Å, 147°). The dinuclear metallocycle is a rhomboid with diagonals of 16.36 Å (Pd···Pd distance) and 13.15 Å (CH_2···CH_2 distance), and its area is 110 Å^2. The angles at the methylene and palladium corners (108° and 88°, respectively) are in the habitual range for this type of bonds.

The analogous platinum [3]catenane (**BPP34C10**)$_2$-(**3b**) could be isolated in 70% yield by reaction of **1**·2PF_6 **BPP34C10** and platinum complex **2b** in CH_3CN at 50 °C. The ^{1}H NMR spectrum showed very similar chemical shifts to those of the analogous palladium catenane. The electrospray ionization mass spectrometry supported the structure, showing signals resulting from the loss of between three and five hexafluorophosphate anions (Figure 4).

Self-Assembly, NMR Study, and Crystal Structure of [3]-Catenanes (DB24C8)$_2$-(3a,b). The addition of 1 equiv of cyclophane **DB24C8** to a 10 mM equimolar solution of ligand **1**·2PF_6 and palladium complex **2a** also produced an intense colored solution. The absorption spectrum showed a new band at λ_{max} = 414 nm. The ^{1}H NMR spectrum of this solution supports the existence of at least three species: metallocycle **3a**, free **DB24C8**, and [3]catenane (**DB24C8**)$_2$-(**3a**) (Figure 5).

(19) (a) Nishio, M.; Hirota, M.; Umezawa, Y. *The CH/π Interaction: Evidence, Nature and Consequences*; Wiley-VCH: Weinheim, Germany, 1998. (b) Oh, M.; Stern, C. L.; Mirkin, C. A. *Inorg. Chem.* **2005**, *44*, 2647. (c) Manimaran, B.; Lai, L.-J.; Thanasekaran, P.; Wu, J.-Y.; Liao, R.-T.; Tseng, T.-W.; Liu, Y.-H.; Lee, G.-H.; Peng, S.-M.; Lu, K.-L. *Inorg. Chem.* **2006**, *45*, 8070.

(20) For example, see: (a) Ashton, P. R.; Ballardini, R.; Balzani, V.; Credi, A.; Gandolfi, M. T.; Menzer, S.; Pérez-García, L.; Prodi, L.; Stoddart, J. F.; Venturi, M.; White, A. J. P.; Williams, D. J. *J. Am. Chem. Soc.* **1995**, *117*, 11171. (b) Asakawa, M.; Ashton, P. R.; Balzani, V.; Brown, C. L.; Credi, A.; Matthews, O. A.; Newton, S. P.; Raymo, F. M.; Shipway, A. N.; Spencer, N.; Quick, A.; Stoddart, J. F.; White, A. J. P.; Williams, D. J. *Chem.—Eur. J.* **1999**, *5*, 860.

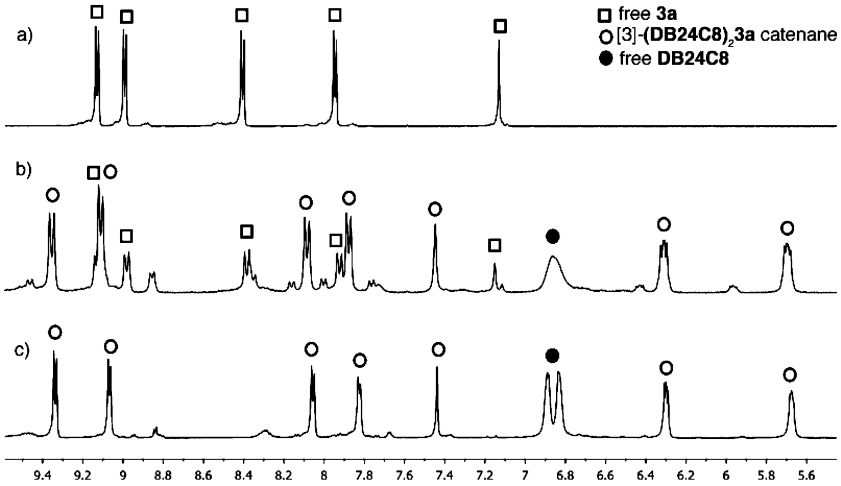

Figure 5. Partial ^{1}H NMR (CD_3CN, 298 K) spectra of (a) metallocycle **3a** (5 mM), (b) **3a** (5 mM) + **DB24C8** (10 mM), and (c) **3a** (5 mM) + **DB24C8** (20 mM).

The addition of an extra 1 equiv of **DB24C8** was necessary to completely shift the equilibrium toward the formation of the [3]catenane. The $BIPY_{ort}$ and $BIPY_{par}$ units are chemically equivalent as a result of the fast exchange on the ^{1}H NMR time scale, and the aromatic protons of the bipyridine systems give rise to four averaged signals. A second dynamic process, fast on the ^{1}H NMR time scale at room temperature, involves the exchange of the inside and alongside catechol rings of **DB24C8**. The methylene protons exhibit a significant downfield shift ($\Delta\delta$ = 0.30 ppm) similar to the shift found in the 1:1 complex between **1**·2PF_6 and **DB24C8**. Thereby, we can assume that the polyether macrocycles encircle the metallocycle around the methylene groups. The diffusion coefficients obtained from DOSY (diffusion-ordered NMR spectroscopy) experiments of a solution of metallocycle **3a** (5 mM) and **DB24C8** (20 mM) showed that the catenane is significantly larger than its components (see Supporting Information). The signals from the metallocycle and the bounded **DB24C8** exhibited the same diffusion coefficient indicating that both components diffuse as a whole. As it could be expected, the signals from the catechol protons of free **DB24C8** in the solution showed a greater diffusion coefficient.

X-ray quality crystals of [3]catenane (**DB24C8**)$_2$-(**3a**) were produced by slow diffusion of isopropyl ether into a solution of **3a** (5 mM) and **DB24C8** (20 mM) in CH_3CN. The X-ray crystal study revealed a [3]catenane structure with the metallocycle **3a** encircled by two C-shaped **DB24C8** molecules around the methylene groups (green macrocycles in Figure 6a,b). Two of the catechol rings are inserted (CAT_{in}) into the metallocycle, while the other two are located outside (CAT_{out}). However, the $\pi-\pi$ stacking system does not comprise the $CAT_{in}\cdots CAT_{in}$ (interplanar distance 3.73 Å) interaction because these units are displaced 2.86 Å from each other in the orthogonal direction to the mean plane defined by the four corners of the metallocycle. Due to this displacement, the $\pi-\pi$ stacking interactions with $BIPY_{par}$ ($CAT_{in}\cdots BIPY_{par}$ 3.26 Å) are weak. In addition to the habitual [C−H···O] bonds between the α-CH bipyridine hydrogens and the oxygen atoms of **DB24C8**, [C−H···O] hydrogen bonds between methylene protons and the oxygen atoms of the polyether chain are also detected. Surprisingly, two external molecules of **DB24C8** with a C-shaped conformation are positioned over the Pd(en) corners in a pseudorotaxane motif (red macrocycles in Figure 6a,b), in which the metallocycle acts as a stopper. The **DB24C8** macroring is held in position by [N−H···O] hydrogen bonds emanating from ethylendiamine; each N−H is involved in a bifurcated H-bonding with two ether oxygen atoms of the polyether macroring. The $\pi-\pi$ stacking system is extended by means $\pi-\pi$ interactions between the catechol rings of each of these external **DB24C8** units (CAT_{ext}) with $BIPY_{par}$ and $BIPY_{ort}$. The mean interplanar separations are $CAT_{ext}\cdots BIPY_{par}$ 3.49 Å and $CAT_{ext}\cdots BIPY_{ort}$ 3.31 Å. The size of the metallocycle is comparable in magnitude to that observed in the case of (**BPP34C10**)$_2$-(**3a**) (16.57 Å × 12.99 Å), although the $BIPY_{par}$ are slightly more twisted (12°) suggesting weaker $\pi-\pi$ stacking interactions as a result of the no alignment of the six aromatic units.

Platinum catenane (**DB24C8**)$_2$-(**3b**) was synthesized and isolated as its hexafluorophosphate salt in 67% yield from metallocycle **3b** and dibenzo-24-crown-8. The ^{1}H NMR spectrum shows similar chemical shifts to that of the palladium analogue.

The crystal structure of (**DB24C8**)$_2$-(**3b**) presents a [3]-catenane structure composed by a square dinuclear metallocycle with almost identical dimensions (16.36 Å × 13.08 Å) to those of (**DB24C8**)$_2$-(**3a**). In this case only two polyether macrocycles in a C-shaped conformation interact with the metallocycle, encircling both methylene groups. As a consequence, $BIPY_{ort}$ is not implicated in $\pi-\pi$ stacking interactions, and its torsion angle increases up to 42° to optimize [C−H···O] bonds between the α-CH bipyridine hydrogens of $BIPY_{ort}$ and the oxygen atoms of **DB24C8** ([H···O] and [C···O] distances and [C−H···O] angle are 2.16, 2.98 Å and 144°).

Reversible Catenation of (DB24C8)$_2$-(3a). It is known that dibenzo-24-crown-8 forms a stable complex with a potassium ion,[21] so we decided to explore the possibility of reverting the formation of (**DB24C8**)$_2$-(**3a**) and monitored this by ^{1}H NMR. Thus, when KPF_6 is added to a yellow colored solution of the catenane, the color vanished as the catenane is dissociated into metallocycle **3a** and the complex between potassium and the crown ether. The ^{1}H NMR spectrum shows clearly the disappearance of the catenane and the appearance of metallocycle

(21) Takeda, Y.; Kudo, Y.; Fujiwara, S. *Bull. Chem. Soc. Jpn.* **1985**, *58*, 1315.

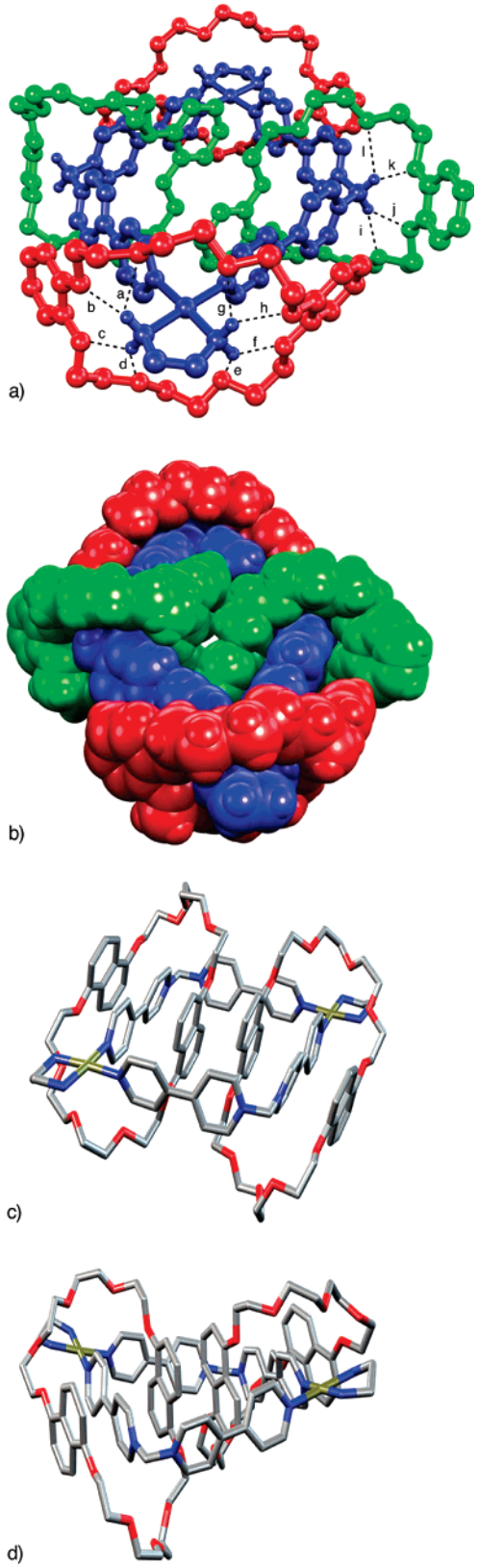

Figure 6. Crystal structure of (a) [3]catenane (**DB24C8**)$_2$-(**3a**) showing [C−H···O] and [N−H···O] hydrogen bonds. [H···O] and [C···O] or [N···O] distances and [C−H···O] angle: a 2.28, 3.08 Å, 145°; b 2.19, 2.90 Å, 134°; c 2.17, 2.95 Å, 142°; d 2.56, 3.23 Å, 131°; e 2.31, 3.07 Å, 140°; f 2.15, 2.86 Å, 134°; g 2.64, 3.32 Å, 131°; h 2.23, 2.99 Å, 139°; i 2.83, 3.53 Å, 128°; j 2.13, 3.05 Å, 154°; k 2.72, 3.03 Å, 99°; l 2.27, 3.18 Å, 152°. (b) Space-filling representation of [3]catenane (**DB24C8**)$_2$-(**3a**). (c) [3]-(**DN38C10**)$_2$-(**3a**)catenane. (d) [3]catenane (**DN38C10**)$_2$-(**3b**). Solvent molecules, counterions, and hydrogen atoms have been omitted for clarity.

3a (Figure 7a−c). This process can be reversed by titration with 18C6 that forms a stronger complex with potassium[22] than **DB24C8** and freeing **DB24C8** rings which then reself-assemble into the catenane (Figure 7d).[23] Particularly worthy of note is the fact that the singlet for amine protons is shifted downfield by 0.10 ppm, suggesting that **DB24C8** is positioned over the metal corners also in solution. A similar shift ($\Delta\delta = 0.30$ ppm) was observed when 2 equiv of **DB24C8** were added to a solution of the platinum catenane (**DB24C8**)$_2$-(**3b**) in CD_3CN.

Self-Assembly, NMR Study, and Crystal Structure of the [3]Catenanes (DN38C10)$_2$-(3a,b). The ^{1}H NMR spectrum recorded in CD_3CN at 298 K for [3]catenane (**DN38C10**)$_2$-(**3a**) self-assembled from **1**·2PF$_6$, **DN38C10**, and **2a** is characterized by line broadening, a phenomenon that would suggest the existence of slow dynamic processes on the ^{1}H NMR time scale. Then, the spectrum was recorded at 250 K, but its complexity prevented any analysis. Probably, at 250 K the circumrotation movements are slow so that BIPY$_{par}$ and BIPY$_{ort}$ and inside (NAPH$_{in}$) and alongside (NAPH$_{out}$) naphthalene rings are nonequivalent. Moreover, the introduction of two 1,5-naphthalene units into the metallocycle results in the inequivalence of the 16 protons of BIPY$_{par}$ and BIPY$_{ort}$ and also the 6 protons of the naphthalene rings. These facts in addition to the relative orientations of the two π-rich components inside the metallocycle cavity can explain the complex spectrum. Fortunately, characterization by X-ray diffratometry was possible (Figure 6c). The solid-state structure shows the expected [3]catenane topology with six aromatic systems in a stack: NAPH$_{out}$/BIPY$_{par}$/NAPH$_{in}$/NAPH$_{in}$/BIPY$_{par}$/NAPH$_{out}$ (interplanar separations (Å) 3.48, 3.38, 3.48, and angles 5°, 0°, 0°, respectively). In addition, [C−H···O] and [N−H···O] hydrogen bonds between methylene protons, α-CH bipyridinium hydrogens and amine protons and the oxygen atoms of the polyether chain are also observed. Platinum catenane [(**DN38C10**)$_2$-(**3b**)]·8PF$_6$ was synthesized in 72% yield following the described procedures for previous platinum catenanes. Although its ^{1}H NMR spectrum is very complex, the [3]catenane could be characterized by MS spectrometry and X-ray crystallographic analysis. ESI high-resolution mass spectrometry revealed a peak resulting from the loss of three PF$_6$ anions. X-ray analysis of single crystals of the [3]catenane (**DN38C10**)$_2$-(**3b**) obtained by vapor diffusion of ethyl ether into acetonitrile solution at room temperature corroborated the proposed structure (Figure 6d). The π stack NAPH$_{out}$/BIPY$_{par}$/NAPH$_{in}$/NAPH$_{in}$ is slightly more distorted than that in the palladium analogue (interplanar separations (Å) 3.64, 3.43, 3.71, and angles 8°, 6°, 2°). Finally, in addition to [C−H···O] and [N−H···O] hydrogen bonds, there are [C−H···π] interactions between the pyridine rings of BIPY$_{ort}$ and the protons of the NAPH$_{in}$ ([H···O] and [C···O] distances and [C−H···O] angles are 2.65 Å and 3.52 Å, 156°). It is particularly interesting the conformation of the diplatinum metallocycle. In this case two diametrically opposite corners of the rhomboid are out of plane, so the metallocycle shows a puckered conformation such that the angles between planes are 34° and 29° for the two planes defined by PtCH$_2$Pt corners and the two planes defined by CH$_2$PtCH$_2$, respectively. While (**DN38C10**)$_2$-(**3a**) only has an inversion center, (**DN38C10**)$_2$-(**3b**) has a C_2 axis perpendicular to the mean plane defined by

(22) Frensdorff, H. K. *J. Am. Chem. Soc.* **1971**, *93*, 600.
(23) Gibson, H. W.; Wang, H.; Slebodnick, C.; Merola, J.; Kassel, W. S.; Rheingold, A. L. *J. Org. Chem.* **2007**, *72*, 3381.

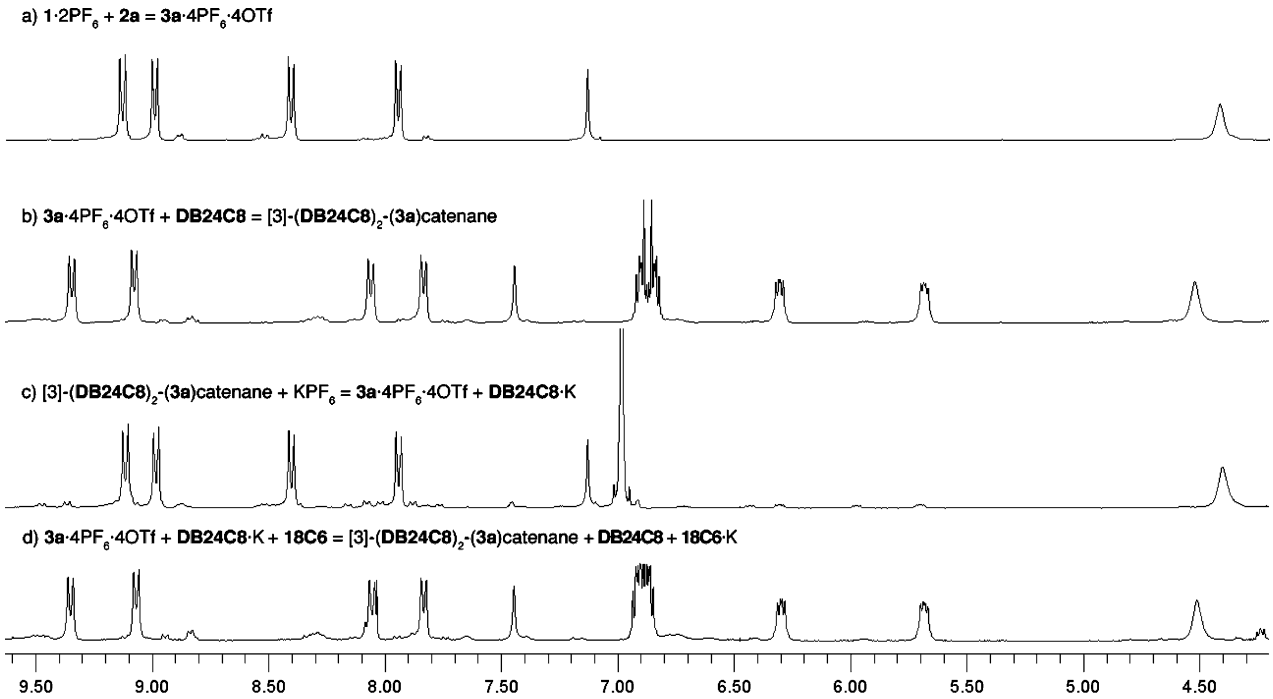

Figure 7. ^{1}H NMR (CD_3CN, 300 MHz, 298 K) spectra of (a) metallocycle **3a** (5 mM), (b) solution (a) + **DB24C8** (20 mM), (c) solution (b) + KPF_6 (20 mM), (d) solution (c) + 18C6 (20 mM).

the four corners of the metallocycle as a consequence of the different relative orientation of the $NAPH_{in}$ units. Thus, while the C(1)−C(5) vectors of $NAPH_{in}$ units are parallel in the palladium catenane, those from the (**DN38C10**)$_2$-(**3b**) are not (Figure 6d).

Conclusions

In summary, a very efficient metal-directed self-assembly of [3]catenanes in combination with $\pi-\pi$ interactions has been described. Ligand **1**·2PF_6 threads through the cavity of **DB24C8** to generate a [2]pseudorotaxane that is stabilized principally by hydrogen-bonding interactions. Platinum metallocycle **3b**·8PF_6 was synthesized (75% yield) by a thermodynamically driven self-assembly reaction at 50 °C to take advantage of the "molecular lock" strategy. The reported catenanes are composed of a dinuclear molecular square bridged by ligand **1**·2PF_6 interpenetrated by two polyether macrorings. X-ray crystallography in combination with NMR studies showed that $\pi-\pi$ stacking and [C−H···π] interactions in addition to [C−H···O] hydrogen bonds are the noncovalent forces that stabilize the [3]catenanes. The solid-state structure of catenane (**DB24C8**)$_2$-(**3a**) revealed that the Pd(en) corners of metallocycle are capped with two additional polyether cyclophanes to form a supramolecular complex composed of eight components. Finally, the catenation process of (**DB24C8**)$_2$-(**3a**) can be switched off and on in a controllable manner by successive addition of KPF_6 and 18-crown-6.

Experimental Section

Reagents and Materials. Cyclophanes **BPP34C10**[24] and **DN38C10**[25] were prepared according to published procedures.

All other reagents were of analytical grade and were used as received. Milli-Q water was purified with a Millipore Gradient A10 apparatus. Merck 60 $HF_{254+366}$ foils were used for thin layer chromatography, and Merck 60 (230−400 mesh) silica gel was used for flash chromatography. NMR spectra were obtained in a Bruker Avance 300 or a Bruker Avance 500 spectrometer equipped with a dual cryoprobe for ^{1}H and ^{13}C or a BBI probe for low-temperature experiments. Diffusion coefficients from DOSY experiments were referenced using an arbitrary value 8.32×10^{-9} m^2/s for the CH_3CN signal in CD_3CN at 298 K. Mass spectrometry experiments were carried out in a Fision VG-Quattro spectrometer for low-resolution FAB using thioglycerol as matrix and an LC-Q-q-TOF Applied Biosystems QSTAR Elite spectrometer for low- and high-resolution ESI. UV−vis spectra were obtained using a Perkin-Elmer Lambda 900 spectrometer. Melting points were measured using a Stuart Scientific SMP3 apparatus. Elemental analyses were obtained in a ThermoQuest Flash EA 1112 analyzer.

Crystal Structure Analysis: The structures were solved by direct methods and refined with the full-matrix least-squares procedure (SHELX-97)[26] against F^2. The X-ray diffraction data were collected on a Bruker X8 APEXII or a Bruker SMART 1k diffractometer. Hydrogen atoms were placed in idealized positions with $U_{eg}(H) = 1.2U_{eg}(C)$ and were allowed to ride on their parent atoms.

1,1′-Methylenebis-4,4′-bipyridinium Bis(hexafluorophosphate) (1·2PF$_6$). A solution of 4,4′-bipyridine (4.45 g, 28.5 mmol) and CH_2Br_2 (2.0 mL, 28.5 mmol) in CH_3CN (40 mL) was refluxed for 4d. After cooling to room temperature, the yellow precipitate was filtered and washed with CH_3CN and ethyl ether to afford a solid which was dissolved in water (100 mL). An excess of NH_4PF_6 was added to the solution until no further precipitation was observed. The white solid was filtered and washed with water to afford **1**·2PF_6 (8.74 g, 91%); mp = 242−245 °C (decomp). ^{1}H NMR (500 MHz, CD_3CN): 7.08 (2H, s), 7.97 (4H, d, J = 6.4 Hz), 8.54 (4H, d, J = 7.0 Hz), 8.91 (4H, d, J = 6.4 Hz), 9.10 (4H, d, J = 7.0 Hz). ^{13}C NMR (125 MHz, CD_3CN): 77.9 (CH_2), 122.9 (CH), 128.0 (CH), 141.3 (C), 146.6 (CH),

(24) Anelli, P. L., et al. *J. Am. Chem. Soc.* **1992**, *114*, 193.
(25) Amabilino, D. B.; Ashton, P. R.; Balzani, V.; Boyd, S. E.; Credi, A.; Lee, J. Y.; Menzer, S.; Stoddart, J. F.; Venturi, M.; Williams, D. J. *J. Am. Chem. Soc* **1998**, *120*, 4295.
(26) Sheldrick, G. M. *SHELX-97, An Integrated System for Solving and Refining Crystal Structures from Diffraction Data*; University of Göttingen: Germany, 1997.

152.3 (CH), 158.9 (C). MS (FAB) *m/z* 471.1 $[M - PF_6]^+$. Anal. Calcd $C_{21}H_{12}F_{12}N_4P_2$: C, 40.92; H, 2.94; N, 9.09. Found: C, 41.01; H, 2.93; N, 8.96.

Metallocycle 3a·4OTf·4PF$_6$. To a solution of ligand **1**·2PF_6 (0.012 g, 0.020 mmol) in CD_3CN (2.0 mL) Pd(en)OTf_2 (0.011 g, 0.024 mmol) was added. ^{1}H NMR (500 MHz, CD_3CN): 2.80 (8H, br s), 4.33 (8H, br s), 7.05(4H, s), 7.86 (8H, d, J = 6.8 Hz), 8.32 (8H, d, J = 7.0 Hz), 8.91 (8H, d, J = 6.8 Hz), 9.05 (8H, d, J = 7.0 Hz). ^{13}C NMR (125 MHz, CD_3CN): 47.8 (CH_2), 78.3 (CH_2), 126.2 (CH), 128.5 (CH), 144.9 (C), 147.1 (CH), 154.0 (CH), 155.7 (C).

Metallocycle 3b·8PF$_6$. A solution of ligand **1**·2PF_6 (0.200 g, 0.325 mmol) and Pt(en)OTf_2 (0.244 g, 0.441 mmol) in CH_3CN (32 mL) was heated at 50 °C for 7d. Upon cooling to room temperature, ether (350 mL) was added and the solid formed was filtered and washed with ether to afford **3b**·4PF_6·4OTf (283,6 mg, 75%). A suspension of this material (0.240 g, 0.103 mmol) and Amberlite CG-400 (2.40 g) in water (20 mL) was stirred at room temperature for 24 h. The resin was removed by filtration, and an excess of KPF_6 was added to the filtrate until no further precipitation was observed. The solid was filtered to yield **3b**·8PF_6 (0.208 g, 87%) as a white solid. Mp = 232−235 °C (decomp). ^{1}H NMR (500 MHz, CD_3CN): 2.80 (8H, br s), 5.03 (8H, br s), 7.11(4H, s), 7.91 (8H, d, J = 6.9 Hz), 8.41 (8H, d, J = 7.1 Hz), 8.94 (8H, d, J = 6.9 Hz), 9.07 (8H, d, J = 7.1 Hz). ^{13}C NMR (125 MHz, CD_3CN): 48.7 (CH_2), 78.4 (CH_2), 126.7 (CH), 128.5 (CH), 144.9 (C), 147.0 (CH), 154.7 (CH), 155.6 (C). HRMS *m/z* (ESI) calcd for $[M - 3PF_6]^{3+}$ 629.0642, found 629.0597; calcd for $[M - 4PF_6^-]^{4+}$ 435.5569, found 435.5574; calcd for $[M - 5PF_6^-]^{5+}$ 319.4526, found 319.4538. Anal. Calcd $C_{46}H_{52}F_{48}N_{12}P_8Pt_2$·3$H_2O$: C, 23.24; H, 2.46; N, 7.07. Found: C, 23.25; H, 2.18; N, 6.80.

General Procedure for the Preparation of Palladium [3]Catenanes. To a solution of ligand **1**·2PF_6 (0.012 g, 0.020 mmol) and Pd(en)OTf_2 (0.011 g, 0.024 mmol) in CD_3CN (2.0 mL), the corresponding cyclophane, **BPP34C10** (0.020 mmol), **DB24C8** (0.040 mmol), or **DN38C10** (0.020 mmol), was added.

[3]Catenane (BPP34C10)$_2$-(3a). ^{1}H NMR (500 MHz, CD_3CN, 237 K): 2.86 (8H, s), 3.23−4.25 (64H, m), 4.57 (4H, s), 4.69 (4H, s), 6.11 (8H, s), 7.12 (4H, s), 7.27 (4H, br s), 7.70 (4H, br s), 8.02 (4H, d, J = 6.5 Hz), 8.41 (4H, d, J = 6.7 Hz), 8.83 (4H, br s), 8.89 (4H, br s), 9.22 (4H, d, J = 6.5 Hz), 9.33 (4H, d, J = 6.7 Hz). ^{13}C NMR (125 MHz, CD_3CN, 237 K): 47.7 (CH_2), 67.8 (CH_2), 70.0 (CH_2), 77.6 (CH_2), 115.0 (CH), 123.7 (CH), 125.4 (CH), 126.5 (CH), 128.3 (CH), 140.6 (C), 144.7 (C), 145.5 (CH), 147.0 (CH), 150.7 (C), 151.2 (C), 153.0 (CH), 154.0 (CH), 155.6 (C).

[3]Catenane (DB24C8)$_2$-(3a). ^{1}H NMR (500 MHz, CD_3CN, 237 K): 2.91 (8H, s), 3.54 (30H, m), 3.71 − 3.82 (58H, m), 4.09 (23H, m), 4.55 (8H, s), 5.67 (8H, m), 6.30 (8H, m), 6.83−6.89 (21H, m), 7.44 (4H, s), 7.83 (4H, d, J = 5.9 Hz), 8.06 (4H, d, J = 6.7 Hz), 9.07 (4H, d, J = 6.5 Hz), 9.34 (4H, d, J = 6.9 Hz). ^{13}C NMR (125 MHz, CD_3CN, 237 K): 47.9 (CH_2), 68.2 (CH_2), 70.0 (CH_2), 71.1 (CH_2), 71.8 (CH_2), 71.8 (CH_2), 78.5 (CH_2), 113.1 (CH), 114.8 (CH), 121.7 (CH), 122.4 (CH), 125.9 (CH), 126.0 (CH), 144.1 (C), 147.4 (C), 148.4 (CH), 149.4 (C), 153.8 (CH), 153.9 (C).

General Procedure for the Preparation of Platinum [3]Catenanes. A solution of **3b**·4OTf·4PF_6 (30 mg, 12.83 mmol) in CH_3CN (2.6 mL) and the corresponding polyether macrocycle (51.30 mmol) was heated at 50 °C for 7d. After cooling to room temperature, ether (100 mL) was added and the precipitate formed was filtered. This solid was suspended in water (5 mL), and Amberlite CG-400 (400 mg) was added. The mixture was stirred at room temperature for 24 h. The resin was removed by filtration, and an excess of KPF_6 was added to the filtrate until no further precipitation was observed. The solid was filtered to yield the catenane.

[3]Catenane (BPP34C10)$_2$-(3b). Red powder. Yield 70%. Mp = 197−200 °C (decomp). ^{1}H NMR (500 MHz, CD_3CN, 237 K): 2.75 (8H, s), 3.15−4.16 (64H, m), 4.99 (4H, s), 5.11 (4H, s), 6.09 (8H, s), 7.03 (4H, s), 7.17 (4H, br s)*, 7.67 (4H, br s), 7.95 (4H, d, J = 6.5 Hz), 8.37 (4H, d, J = 6.5 Hz), 8.85 (8H, br s), 9.17 (4H, d, J = 6.6 Hz), 9.26 (4H, d, J = 6.7 Hz). ^{13}C NMR (125 MHz, CD_3CN, 237 K): 48.2 (CH_2), 48.6 (CH_2), 66.4 (CH_2), 67.8 (CH_2), 67.9 (CH_2), 70.0 (CH_2), 70.3 (CH_2), 77.7 (CH_2), 115.2 (CH), 124.2 (CH), 125.4 (CH), 127.0 (CH), 128.3 (CH), 140.4 (C), 144.4 (C), 145.9 (CH), 146.9 (CH), 151.2 (C), 152.3 (C). 154.1 (CH), 154.8 (CH), 155.5 (C). HRMS *m/z* (ESI) calcd for $[M - 3PF_6]^{3+}$ 986.5723, found 986.5716; 703.9 $[M - 4PF_6]^{4+}$, 533.9 $[M - 5PF_6]^{5+}$. Anal. Calcd $C_{102}H_{132}F_{48}N_{12}O_{20}P_8Pt_2$: C, 36.07; H, 3.92; N, 4.95. Found: C, 35.84; H, 3.75; N, 5.23.

[3]Catenane (DB24C8)$_2$-(3b). Orange-yellow powder. Yield 67%. Mp = 200−2005 °C (decomp). ^{1}H NMR (500 MHz, CD_3CN): 2.80 (8H, s), 3.75 (16H, s), 3.53−3.59 (32H, m), 4.91 (8H, s), 5.72−5.74 (8H, m), 6.28−6.30 (8H, m), 7.46 (4H, s), 7.81 (4H, d, J = 6.7 Hz), 8.05 (4H, d, J = 7.0 Hz), 9.03 (4H, d, J = 6.9 Hz), 9.38 (4H, d, J = 7.1 Hz). ^{13}C NMR (125 MHz, CD_3CN, 237 K): 48.7 (CH_2), 69.3 (CH_2), 71.1 (CH_2), 71.9 (CH_2), 78.6 (CH_2), 113.3 (CH), 121.7 (CH), 126.0 (CH), 126.5 (CH), 144.3 (C), 147.5 (C), 148.5 (CH), 153.7 (C), 154.7 (CH). HRMS *m/z* (ESI) 1464.3 $[M - 2PF_6]^{2+}$; calcd for $[M - 3PF_6^-]^{3+}$ 927.8706, found 927.8689. Anal. Calcd $C_{94}H_{116}F_{48}N_{12}O_{16}P_8Pt_2$: C, 35.06; H, 3.63; N, 5.22. Found: C, 35.29; H, 3.41; N, 5.49.

[3]Catenane (DN38C10)$_2$-(3b). Violet powder. Yield 72%. Mp = 199−202 °C (decomp). HRMS *m/z* (ESI) 1652.4 $[M - 2PF_6]^{2+}$; calcd for $[M - 3PF_6^-]^{3+}$ 1053.2598, found 1053.2545; 753.4 $[M - 4PF_6]^{4+}$. Anal. Calcd $C_{118}H_{140}F_{48}N_{12}O_{20}P_8Pt_2$·8$H_2O$: C, 37.89; H, 4.20; N, 4.49. Found: C, 37.68; H, 3.83; N, 4.43.

Acknowledgment. This research was supported by Xunta de Galicia (PGIDIT04PXIC10307PN and PGIDIT06PXIB103224PR) and Ministerio de Educación y Cultura (CTQ2006-04728/BQU). V.B. and D.A. thank Ministerio de Educación y Ciencia (FPU program) and Xunta de Galicia, respectively, for predoctoral fellowships.

Supporting Information Available: Complete ref 24, ^{1}H NMR, ^{13}C NMR, and 2D experiments for all compounds, titration curves of pseudorotaxanes (**BPP34C10**)(**1**·2PF_6) and (**DB24C8**)(**1**·2PF_6), and crystallographic files (in CIF format) of **1**·2PF_6, **DB24C8-1**·2PF_6, (**BPP34C10**)$_2$-(**3a**), (**DB24C8**)$_2$-(**3a**), (**DB24C8**)$_2$-(**3b**), (**DN38C10**)$_2$-(**3a**), and (**DN38C10**)$_2$-(**3b**). This material is available free of charge via the Internet at http://pubs.acs.org.

JA074721A